



New FAAH inhibitors based on 3-carboxamido-5-aryl-isoxazole scaffold that protect against experimental colitis

Virginie Andrzejak^a, Giulio G. Muccioli^{b,e}, Mathilde Body-Malapel^c, Jamal El Bakali^a, Madjid Djouina^c, Nicolas Renault^d, Philippe Chavatte^d, Pierre Desreumaux^c, Didier M. Lambert^e, Régis Millet^{a,*}

^a Université Lille Nord de France, ICPAL, EA 4481, IFR114, 3 rue du Professeur Laguesse, BP-83, F-59006 Lille, France

^b Université Catholique de Louvain, Louvain Drug Research Institute, Bioanalysis and Pharmacology of Bioactive Lipids Lab, 72 Avenue E. Mounier (CHAM7230), B-1200 Bruxelles, Belgium

^c Université Lille Nord de France, INSERM U995, Faculté de Médecine, Amphi J & K, IFR114, Boulevard du Professeur Leclercq, F-59045 Lille, France

^d Université Lille Nord de France, Faculté des Sciences Pharmaceutiques et Biologiques, Laboratoire de Chimie Thérapeutique, EA 4481, IFR 114, 3 rue du Professeur Laguesse, BP-83, F-59006 Lille, France

^e Université catholique de Louvain, Louvain Drug Research Institute, Unité de Chimie Pharmaceutique et de Radiopharmacie, 73 Avenue E. Mounier UCL (CMFA7340), B-1200 Bruxelles, Belgium

ARTICLE INFO

Article history:

Received 10 February 2011

Revised 26 April 2011

Accepted 30 April 2011

Available online 6 May 2011

Keywords:

FAAH

Cannabinoids

IBD

Isoxazole

FAAH modeling

ABSTRACT

Growing evidence suggests a role for the endocannabinoid (EC) system, in intestinal inflammation and compounds inhibiting anandamide degradation offer a promising therapeutic option for the treatment of inflammatory bowel diseases. In this paper, we report the first series of carboxamides derivatives possessing FAAH inhibitory activities. Among them, compound **39** displayed significant inhibitory FAAH activity ($IC_{50} = 0.088 \mu\text{M}$) and reduced colitis induced by intrarectal administration of TNBS.

© 2011 Elsevier Ltd. All rights reserved.

1. Introduction

Endocannabinoids (ECs), including anandamide (AEA) and 2-arachidonoylglycerol (2-AG), are arachidonic acid derived bioactive lipids that are biosynthesized on demand, and which, following the activation of both cannabinoid receptors (CB_1 and CB_2) trigger a wide range of biological responses. These physiological effects are transient due to a rapid inactivation of ECs by specific enzymes such as fatty acid amide hydrolase (FAAH) and monoacylglycerol lipase (MAGL).^{1–4}

In the gastrointestinal tract, these endogenous ligands control, notably via CB_1 and/or CB_2 receptor activation, many physiological functions including intestinal motility, secretion and inflammation.⁵ Accordingly, stimulation of cannabinoid receptors directly or indirectly constitutes a promising strategy to treat several gastrointestinal pathologies, especially diseases wherein an inflammatory process is involved such as, for example, inflammatory bowel diseases.

For that matter, increased levels of AEA as well as up-regulation of cannabinoid receptors expression were reported during intestinal inflammation,^{6–8} and described as a protective mechanism to counteract inflammation.⁹ Over the past few years several studies have provided evidence that exogenous agonists acting at CB_1 and/or CB_2 receptors, as well as inhibitors of EC re-uptake and degradation, provide protection against experimental colitis.^{10–12} Indeed, it has been shown that the nonselective cannabinoid receptor agonist HU210 as well as the two selective CB_2 receptor agonist JWH133 and AM1241 are able to significantly reduce inflammation in hapten-induced colitis in mice.¹⁰ Consistent with these results, both genetic and pharmacological blockade of either CB_1 or CB_2 receptor signaling led to a worsening of colitis in these experimental models.¹⁰ Another approach consisting in raising anandamide levels has been successfully applied to reduce intestinal inflammation by using inhibitors of EC membrane transport (VDM11) or FAAH (URB597).¹¹ The involvement of both cannabinoid receptors was confirmed by performing experiments in CB_1 and CB_2 knock out mice.

Targeting FAAH is of particular interest since it increases AEA, and related *N*-acylethanolamines, levels without triggering

* Corresponding author. Tel.: +33 320964374; fax: +33 320964906.

E-mail address: regis.millet@univ-lille2.fr (R. Millet).

psychotropic effects associated with central CB₁ receptor activation.¹³ It is noteworthy that these side effects represent a real curb for the use of CB₁-interacting ligands in therapeutic. Thus, inhibitors of FAAH account for a real option to elicit the pharmacological effects of CB₁ receptor activation, while avoiding CNS side effects.

In this context, we undertook the development of a new series of FAAH inhibitors based on a 3-carboxamido-5-aryl-isoxazole scaffold, which general structure is shown in Figure 1. We chose this template because:

- (i) Amide derivatives represent an extension and an alternative to α -keto-heterocycles (OL-135),¹⁴ aryl carbamates¹⁵ (URB597) and ureas (PF622)¹⁶ usually described as potent FAAH inhibitors;

- (ii) Isoxazole rings have never been described as FAAH inhibitors and the interactions with the enzyme are expected to be different to the one observed with α -ketooxazoles, since it has been shown that small changes in the nature of the heterocycle result in huge differences in activity.¹⁶

The amide function introduced at the C-3 position of the isoxazole was hypothesized to interact with Ser241 of the Ser-Ser-Lys catalytic triad of FAAH and the aryl group in C-5 position, to fill in the wide hydrophobic pocket (acyl binding pocket) of the enzyme.¹⁷ Finally, we introduced different aromatic groups, more or less distant from the carboxamide function at position 3, to complete the structure-activity relationships.

The FAAH inhibitory potential of the newly synthesized compounds was evaluated and our lead was then assayed in the

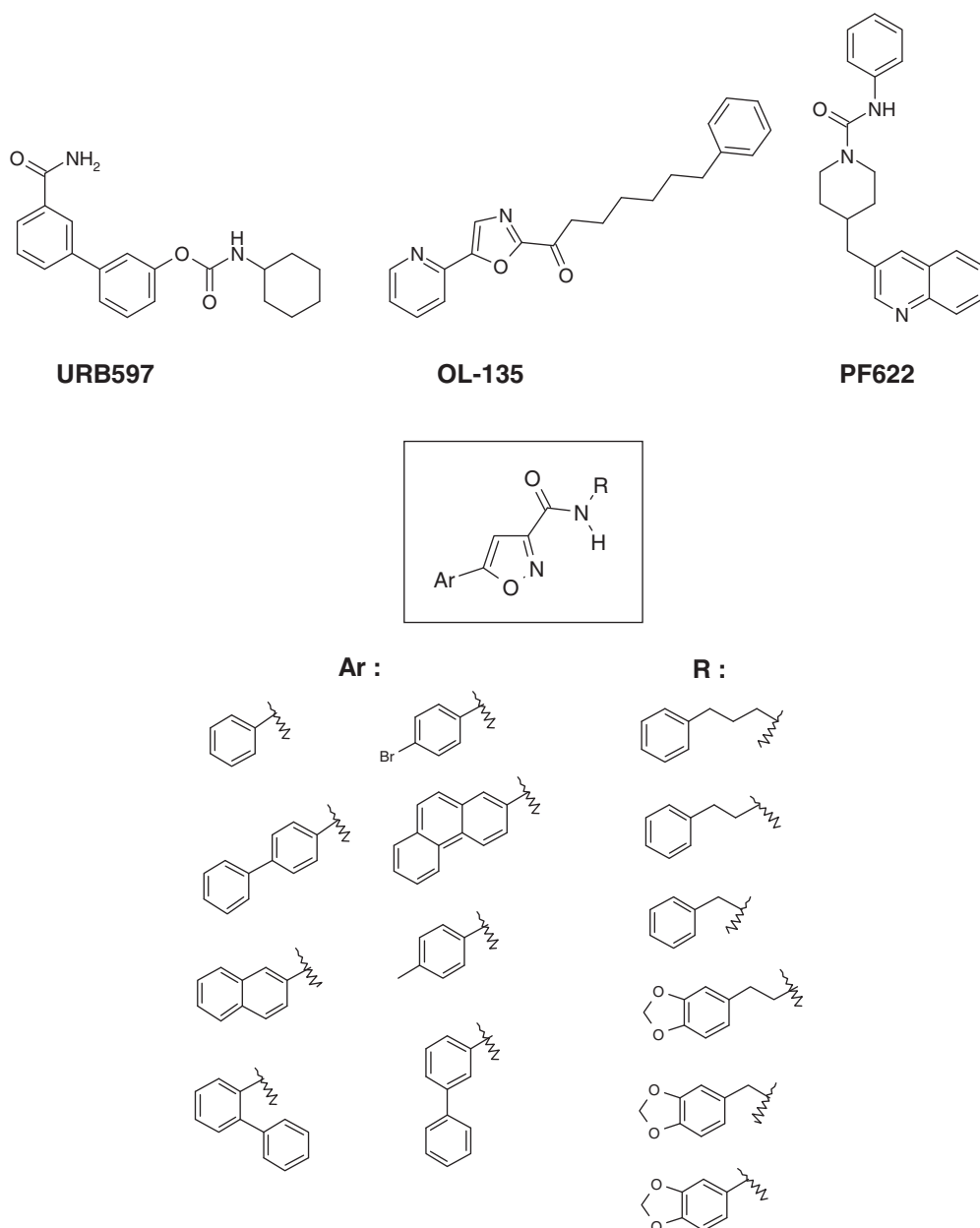
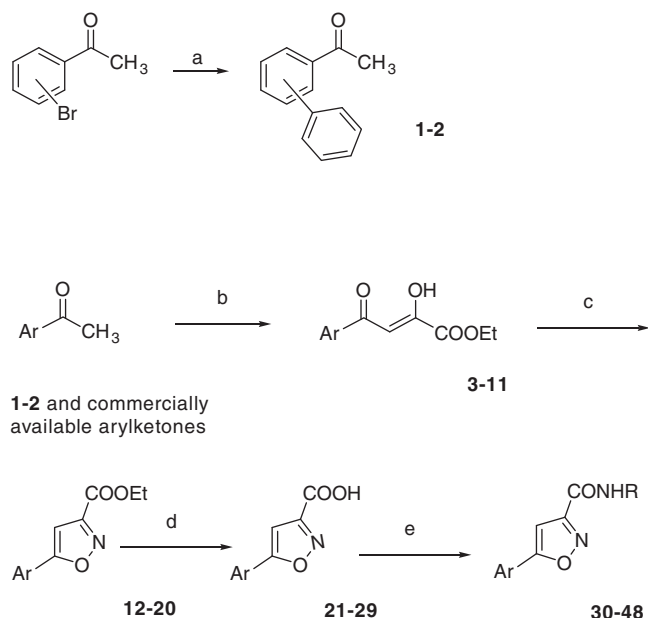


Figure 1. General structure of novel 3-amido-5-aryl-isoxazole derivatives compared to URB597, OL-135 and ureas (compound A).



Scheme 1. Reagents and conditions: (a) phenylboronic acid, K_2CO_3 , DME/ H_2O (1:1), rt, 48 h; (b) diethyl oxalate, sodium ethanolate, EtOH, reflux, 2 h; (c) hydroxylamine hydrochloride, EtOH, reflux, 2 h; (d) sodium hydroxide, EtOH (95%), rt, 24 h; (e) $R-NH_2$, HBTU, HOBt, DIPEA, CH_2Cl_2 , rt, 24 h.

experimental model of TNBS-induced colitis (TNBS: 2,4,6-trinitrobenzene sulfonic acid), allowing the identification of a new FAAH inhibitor endowed with anti-inflammatory properties in the gut.

2. Results and discussion

2.1. Synthesis of inhibitors

The target 3-carboxamido-5-aryl-isoxazoles **30–48** were obtained in four steps from arylketones, as described in Scheme 1. When the aromatic ketones were not commercially available a

preliminary additional step, consisting in a Suzuki coupling reaction, was used (compounds **1** and **2**). Then, arylketones underwent a Claisen condensation to afford 1,3-diketone esters **3–11**, obtained in their enol forms, in variable yields (37–99%). Cyclisation into 3-carboxylate-5-aryl-isoxazole (compounds **12–20**) was carried out by addition of hydroxylamine hydrochloride on 1,3-diketone esters as previously described.¹⁸ The target compounds **30–48** were finally obtained in moderate yields (47–80%), by saponification of the ethyl ester function of compounds **12–21** with sodium hydroxide followed by amidification under peptide coupling conditions (HOBt/HBTU).

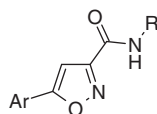
2.2. In vitro pharmacology

The novel 3-carboxamido-5-aryl-isoxazoles have been evaluated for their ability to inhibit the hydrolysis of [3H]-AEA by a recombinant human FAAH preparation.^{19–21} Inhibitory data are summarized in Table 1.

From a structure–activity relationship perspective, compounds can be divided into two series, depending on their aromatic terminal group borne by the carboxamide at C-3 position: compounds **30–36** and **45–46** possess a phenyl terminal group (series A) whereas compounds **37–44** and **47–48** are characterized by a 1,3-benzodioxolyl moiety.

We started our investigations by evaluating the importance of the substituent borne by the amide at C-3. This first part of the study was carried out with a 4-biphenyl at C-5 position since this group generally led to compounds with high affinity for FAAH.¹⁷ Thus, compounds **32**, **39** and **45–48** were synthesized allowing the emergence of some interesting SAR. Indeed, in the series A, the increase of the chain length led to a 200-fold improvement of the activity with IC_{50} values decreasing from 105 μM for **45** (benzyl group), to 0.501 μM for **32** (phenylpropyl group). As for the series B, no significant difference was observed between the activities of compound **47** (1,3-benzodioxolyl) and **48** ((1,3-benzodioxolyl)methyl). More surprisingly, a sharp increase (>1000-fold) of activity was noticed when the (1,3-benzodioxolyl)methyl of compound **48** (IC_{50} = 92.1 μM) was replaced with the (1,3-benzodioxolyl)ethyl moiety (compound **39**, IC_{50} = 0.088 μM). It is noteworthy that when direct comparison was possible, compounds from series

Table 1
Structures and inhibitory activities of compounds **30–48**^a



Compounds	Ar	R	IC_{50} (μM) or FAAH (% inhibition)
30	Phenyl	Phenylpropyl	30.78%
31	4-Bromophenyl	Phenylpropyl	251 \pm 41 μM
32	4-Biphenyl	Phenylpropyl	0.50 \pm 0.1 μM
33	2-Phenanyl	Phenylpropyl	12.6 \pm 1.5 μM
34	2-Naphthyl	Phenylpropyl	38.7%
35	<i>p</i> -Tolyl	Phenylpropyl	125 \pm 31 μM
36	4-Trifluoromethylphenyl	Phenylpropyl	25.1 \pm 6.0 μM
37	Phenyl	2-(Benzo[d][1,3]dioxol-5-yl)ethyl	25.1 \pm 3.7 μM
38	4-Bromophenyl	2-(Benzo[d][1,3]dioxol-5-yl)ethyl	39.8 \pm 5.1 μM
39	4-Biphenyl	2-(Benzo[d][1,3]dioxol-5-yl)ethyl	0.088 \pm 0.004 μM
40	2-Naphthyl	2-(Benzo[d][1,3]dioxol-5-yl)ethyl	10.0 \pm 0.4 μM
41	<i>p</i> -Tolyl	2-(Benzo[d][1,3]dioxol-5-yl)ethyl	79.4 \pm 14 μM
42	4-Trifluoromethylphenyl	2-(Benzo[d][1,3]dioxol-5-yl)ethyl	20.0 \pm 2.2 μM
43	2-Biphenyl	2-(Benzo[d][1,3]dioxol-5-yl)ethyl	2.6%
44	3-Biphenyl	2-(Benzo[d][1,3]dioxol-5-yl)ethyl	43.8 \pm 4.8 μM
45	4-Biphenyl	Benzyl	105.0 \pm 15 μM
46	4-Biphenyl	Phenethyl	70.0 \pm 10 μM
47	4-Biphenyl	Benzo[d][1,3]dioxol-5-yl	57.5 \pm 8.5 μM
48	4-Biphenyl	2-(Benzo[d][1,3]dioxol-5-yl)methyl	92.1 \pm 18 μM

^a Data represent the mean \pm SEM of three experiments performed in duplicate.

B (**37–42**) exhibit higher affinities for FAAH than their counterparts in the series A (**30–36**). This significant difference of activity is probably due to the ability of the 1,3-benzodioxolyl group to establish hydrogen bonds with the protein.

These data demonstrate that the activity is very sensitive to the nature of the terminal aromatic group borne by the carboxamide at position 3, as well as the length of the carbon chain linking this terminal group to the heterocyclic core. Consequently, for the second part of the study, we decided to retain the phenylpropyl and (1,3-benzodioxolyl)ethyl group as 3-carboxamido substituent, for the series A and B, respectively.

Next, we sought to evaluate the impact of the aromatic substituent at C-5 position of the isoxazole ring by replacing the 4-biphenyl moiety by other aromatic groups (compounds **30–31**, **33–38**, and **40–42**). Unfortunately, regardless to the C-3 substituent, this strategy resulted in compounds with only moderate or no affinity for FAAH. Indeed, introducing bromine, methyl or trifluoromethyl in place of one phenyl of the 4-biphenyl group (e.g., compare compounds **38**, **41** and **42** vs **39**) resulted in a drastic reduction in FAAH inhibition. Analogously, the rigidification of the 4-biphenyl into 2-phenantryl as well as its replacement with a phenyl or a 2-naphthyl group did not improve FAAH activity. Finally, we replaced the 4-biphenyl moiety by its position isomers in order to study the importance of the biphenyl substitution. By comparison with compound **39** ($IC_{50} = 0.088 \mu\text{M}$), this modification resulted in a strong reduction of the affinity as for the 3-biphenyl group (**43**, $IC_{50} = 43.8 \mu\text{M}$), while the 2-biphenyl (**44**) completely abolished FAAH affinity. These data demonstrate that at C-5 position of the isoxazole ring, the 4-biphenyl substitution is optimal for FAAH activity. Of note, no MAGL inhibitory activity was detected for our lead compound (**39**) when assayed at concentrations up to $30 \mu\text{M}$ (i.e., at a concentration more than 300 times higher than its FAAH IC_{50}).

In conclusion, compound **39**, characterized by a 4-biphenyl group at C-5 position and a (1,3-benzodioxolyl)ethyl carboxamido substituent at position 3 of the isoxazole ring, was found to be the most potent FAAH inhibitor of our series with an IC_{50} value of $0.088 \mu\text{M}$. Thus, we next conducted in silico modeling studies to enhance our understanding of the mechanism of action of **39**.

2.3. In silico study

Docking procedures in the FAAH enzyme have been performed in order to identify key interactions of compound **39** with the enzyme in comparison with the binding mode of OL-135, a reference inhibitor. Thus the holo-enzyme FAAH co-crystallized with OL-135 covalent inhibitor has been used as the target (1WJ1 PDB entry).²⁵

Prior GOLD docking procedures²⁶ have permitted to recover the ten top-10 solutions of OL-135, with the GoldScore scoring function, within a 2 \AA RMSd (data not shown here) in comparison with its co-crystallized conformation. As this is a covalently bound molecule, this process assumed a modified ligand by docking its intermediate-type diol conformation and replacing the Ser241 by an Alanine residue in order to mimic the electrophile addition of the serine hydroxyle group by the ligand carbonyl.²⁷ As the binding mechanism of **39** is not known, the docking of the compound was tested in both wild-type and alanine-mutated targets from its initial carboxamido or amino-methanediol forms, respectively. In both cases, the best GoldScore solutions of the most representative binding mode are so similar that only the carboxamide form of **39** is represented as docked in the wild-type FAAH receptor (Fig. 2).

In comparison with OL-135, the polar isoxazole-carboxamide moiety of compound **39** fits in the oxyanion hole establishing hydrogen bonds Lys142–carbonyl and Ile138–isoxazole. Nevertheless, it makes the benzodioxol chain binding further in a region of the entrance cavity not occupied by OL-135. Note that the docking results reflect some of the structure–affinity relationships found in the inhibition assays. Indeed, the optimal length for the linker of the 2-(benzo[d][1,3]dioxol-5-yl) substituent is of 2 methylenes, compared to one methylene (compound **48**) of none (compound **47**). In addition, the hydrogen bond acceptors of benzodioxol allow an additional hydrogen bond with Gln273—compared to the phenyl of compound **32**—which could explain the significant gain of binding. Also, as for the OL-135, the more hydrophobic group—4-biphenyl—is reasonably fitting in the ABP (acyl binding pocket). However, in contrast with the acylphenyl chain of OL-135 which is flexible enough to fit toward the membrane access channel, the intrinsic rigid conformation of

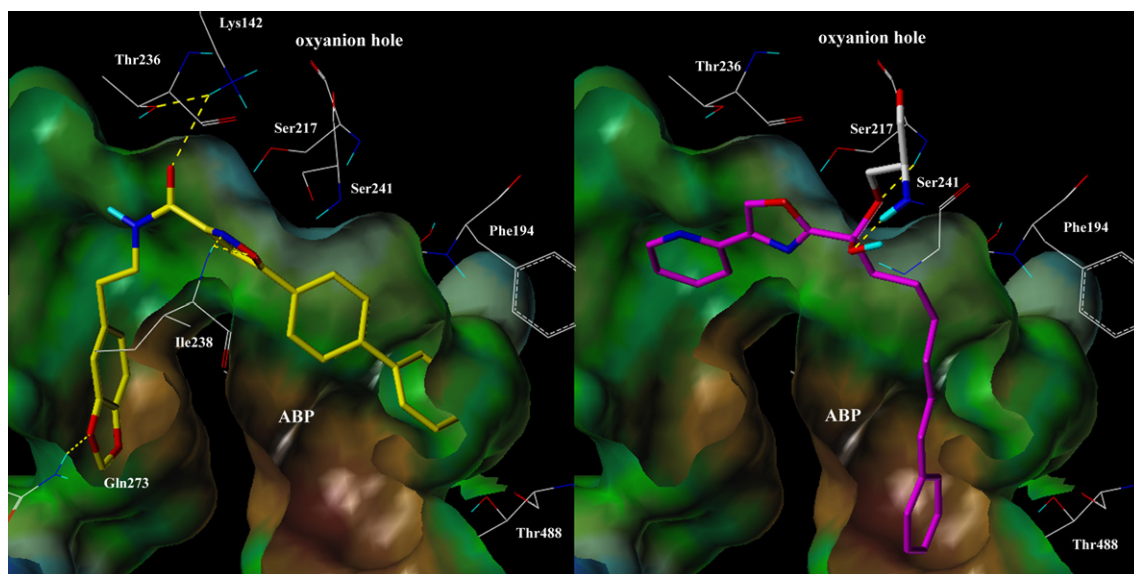


Figure 2. In silico binding mode of compound **39**. The best docking solution of the compound **39** (left) is compared to the co-crystallized OL-135 reference compound (right). They are represented as sticks in yellow and magenta, respectively, as well as the covalently bound Ser241 in white. The intermolecular hydrogen bonds are displayed in yellow dashed lines whereas intermolecular van der Waals interactions are implicitly associated to the shape of the solvent-accessible binding site, colored from blue for polar areas to brown for lipophilic areas. Graphical inspection of models was performed on the SYBYL 6.9.2 software.²⁸

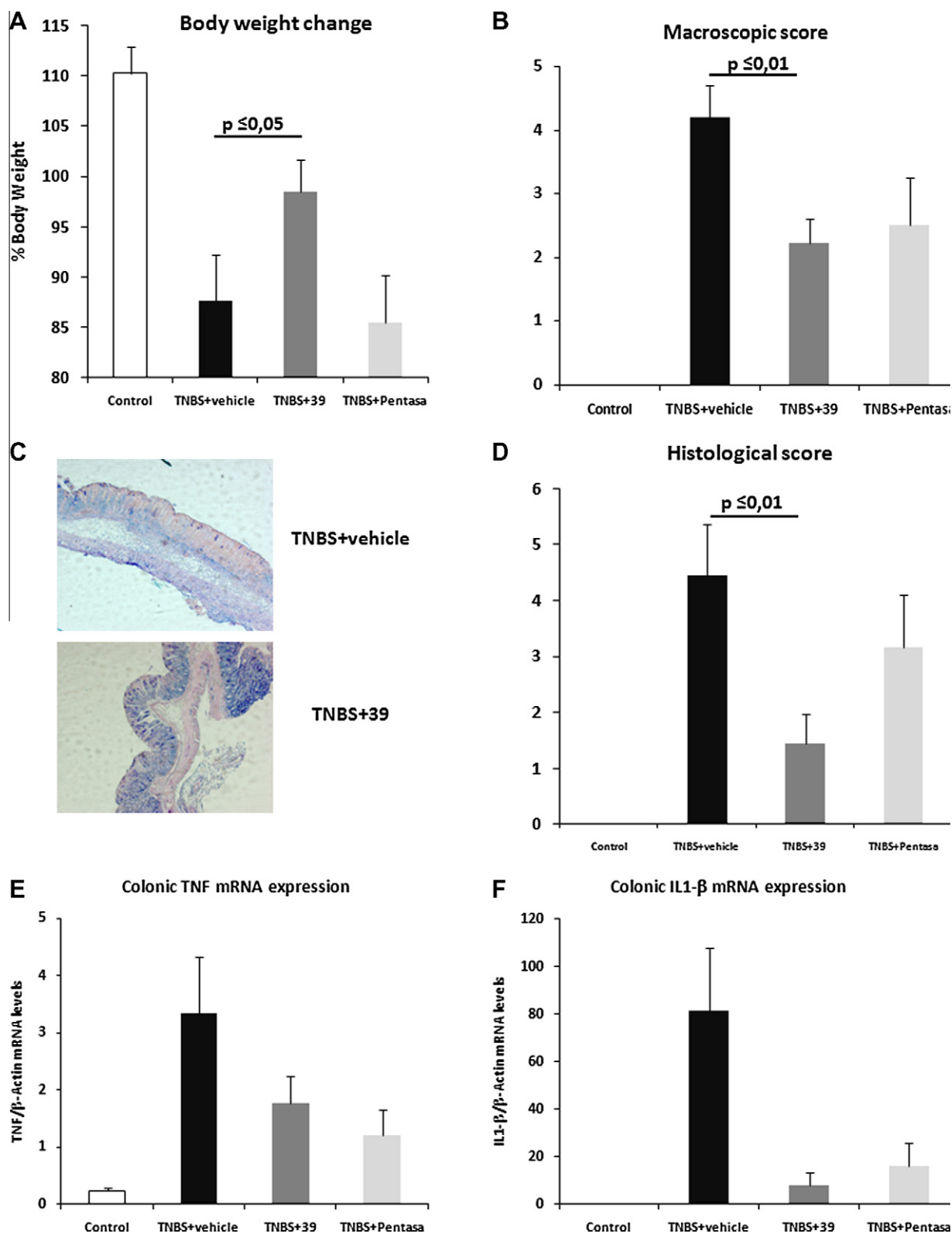


Figure 3. The FAAH inhibitor **39** protects against TNBS-induced colitis. (A) Changes in body weight at the day of sacrifice as compared with the day of colitis induction. (B) Macroscopic score of the colonic tissue according to Wallace criteria. (C) MGG-stained colonic tissue of mice challenged with TNBS and treated with vehicle or **39**. Histology of vehicle treated mice showed massive infiltration of mononuclear cells as well as destruction of crypt architecture (top); histology of **39**-treated mice showed almost normal colonic tissue with minimal infiltration of mononuclear cells (bottom). Original magnification, $\times 20$. (D) Histological score of the colonic tissue of the mice according to Ameho criteria. (E) and (F) Effect of **39** on TNF and IL-1 β mRNA expression levels.

4-biphenyl constrains the docking of the terminal phenyl in a sub-pocket thus establishing an orthogonal π - π aromatic interaction with Phe194. The bent shape between the oxyanion hole and

ABP regions does not allow the suitable fit of 2-biphenyl (compound **43**) and 3-biphenyl (compound **44**) which translates in inactive compounds in the inhibition tests.

2.4. In vivo pharmacology

To demonstrate the potential of compound **39** as an in vivo FAAH inhibitor we investigated the effect of our lead compound in the mouse model of TNBS-induced colitis. Thus, compound **39** was administered intraperitoneally once daily at the dosage of 10 mg/kg, starting three days before colitis induction. 5-Aminosalicylic acid (5-ASA, Pentasa) granules (the standard first-line therapy for patients with mild-to-moderate ulcerative colitis), mixed in food at the dosage of 150 mg/kg, and provided ad libitum during all the course of the experiment, was used as anti-inflammatory positive control.²² Mice were euthanized three days after TNBS administration and parameters reflecting the degree of inflammation were assessed.

Before euthanasia, the body weight loss was evaluated. As can be seen from Figure 3A, daily treatment with compound **39** significantly reduced body weight loss generally observed during the development of TNBS colitis. The colon of each mouse was then examined and damages were assessed by a semi-quantitative scoring system.²³ As shown in Figure 3B, **39** induced a decrease in colitis macroscopic scores of the same magnitude as the positive control 5-ASA (47%, 2.2 ± 0.4 vs 4.2 ± 0.5 , $p \leq 0.01$). Moreover, whereas untreated mice exhibited destruction of crypt architecture and infiltration of mononuclear cells in the colonic lamina propria, mice treated with compound **39** exhibited only minor epithelial damage or cellular infiltration (Fig. 3C).

This protective effect was confirmed by the histological colitis scores (Fig. 3D).²⁴ Indeed, **39** led to 68% decrease of the colitis histological score as compared to the vehicle (1.4 ± 0.5 vs 4.4 ± 0.9 , $p \leq 0.01$). Finally, the quantification of colonic TNF and IL1- β mRNA expression, two cytokines widely involved in the inflammatory response leading to epithelial injury, showed that systemic administration of **39** induced a potent anti-inflammatory effect, comparable to the one observed after treatment with 5-ASA (Fig. 3E and 3F).

Taken together, these data clearly indicate that our new FAAH inhibitor is endowed with potent anti-inflammatory properties in the gut. Our work is consistent with two previous reports that showed that genetic ablation (FAAH^{-/-} mice) or pharmacological inhibition of FAAH (using URB597) could provide protection against experimental colitis.^{10,11} Here, we show that this anti-inflammatory effect can be obtained with another class of FAAH inhibitor (different from the carbamate derivative URB597), which validate FAAH as a promising therapeutic target for the treatment of colitis.

3. Conclusion

In this paper, we described the first series of carboxamide derivatives that present FAAH activities. Based on 3-carboxamido-5-aryl-isoxazole scaffolds, the compound presented SAR different from α -ketoheterocycle series. Indeed, different aromatic substituents were introduced in C-5 position of the isoxazole and the best activities were found with a 4-biphenyl group. The importance of the substituent borne by the nitrogen atom of the amide function was investigated and the best inhibitory capacities were obtained when the substituent was the (1,3-benzodioxolyl)ethyl group. Docking studies revealed no interaction with Ser241, suggesting a different binding mode compared to URB597 or OL-135.

In this series, compound **39** inhibits FAAH with an IC₅₀ value of 0.088 μ M, without affecting MAGL activity, and efficiently reduces the inflammation and colon damage in a model of TNBS-induced colitis in mice, showing evidence that FAAH inhibitors are promising target for the Inflammatory Bowel Diseases (IBD) treatment.

4. Experimental

4.1. Chemistry

All commercial reagents and solvents were used without further purification. Analytical thin-layer chromatography was performed on pre-coated Kieselgel 60F254 plates (Merck); the spots were located by UV (254 and 366 nm) and/or with iodine. Silica gel 60 230–400 mesh purchased from Merck was used for column chromatography. Preparative thick-layer chromatography (TLC) was performed using silica gel from Merck, the compounds were extracted from the silica using cyclohexane/AcOEt (7:3, v/v). All melting points were determined with a Büchi 535 capillary apparatus and remain uncorrected. ¹H NMR spectra were obtained using a Brücker 300 MHz spectrometer, chemical shift (δ) were expressed in ppm relative to tetramethylsilane used as an internal standard, *J* values are in hertz. All compounds were analyzed by HPLC–MS on a HPLC combined with a Surveyor MSQ (Thermo Electron) equipped with an APCI-source. All tested compounds showed a purity of >96% in APCI+ mode. Elemental analyses for target compounds were performed by the 'Service Central d'Analyses' at the CNRS, Vernaison (France) and the data were within $\pm 0.4\%$ of the theoretical values.

4.1.1. General procedure for the preparation of 1-(biphenyl-2-yl)ethanone (**1**) and 1-(biphenyl-3-yl)ethanone (**2**)

2'- or 3'-Bromoacetophenone (10.05 mmol, 1 equiv) and phenylboronic acid (12.04 mmol, 1.2 equiv) were dissolved in a mixture of DME (30 mL) and H₂O (30 mL). Then, K₂CO₃ (15.08 mmol, 1.5 equiv) and tetrakis(triphenylphosphine)palladium (0.05 mol, 0.005 equiv) were added and the mixture was refluxed for 48 h. After cooling to room temperature, the suspension was filtered off and the filtrate was extracted with CH₂Cl₂. The resulting organic layer was dried over MgSO₄ and concentrated under reduced pressure. The resulting residue was purified by silica gel column chromatography (cyclohexane/AcOEt, 6:4) to afford the corresponding derivatives **1** and **2**.

4.1.1.1. 1-(Biphen-2-yl)ethanone (1**).** Brown oil (31%); ¹H NMR (DMSO-*d*₆) δ 7.60–7.28 (m, 9H), 2.09 (s, 3H). LC/MS (APCI⁺) *m/z* 197.3 (MH⁺).

4.1.1.2. 1-(Biphen-3-yl)ethanone (2**).** Yellow oil (17%); ¹H NMR (DMSO-*d*₆) δ 8.15 (s, 1H), 7.92–7.36 (m, 8H), 2.61 (s, 3H). LC/MS (APCI⁺) *m/z* 197.3 (MH⁺).

4.1.2. General procedure for the preparation of ethyl 2-hydroxy-4-oxo-4-aryl-but-2-enoate (**3–11**)

To a stirred solution of sodium ethanolate freshly prepared from Na (66.04 mmol, 2 equiv) in 50 mL of absolute EtOH, were added dropwise, at 50 °C, the aryl ketone (33.02 mmol, 1 equiv) and the diethyl oxalate (66.04 mmol, 2 equiv) diluted in 30 mL of absolute ethyl alcohol. The mixture was refluxed for 2 h. The solvent was evaporated and the obtained residue was taken up in an aqueous solution of hydrochloric acid (1N) and stirred for 1 h. Then, it was extracted with AcOEt and washed with distilled water. The organic layer was dried over MgSO₄ and the solvent removed. Finally, the residue was triturated in cyclohexane to give compounds **3–11**.

4.1.2.1. Ethyl 2-hydroxy-4-oxo-4-phenyl-2-butenate (3**).** Orange oil (75%); ¹H NMR (DMSO-*d*₆) δ 10.68 (s, 1H), 8.02 (d, 2H, *J* = 7.7 Hz), 7.67 (t, 1H, *J* = 7.9 Hz), 7.54 (t, 2H, *J* = 7.8 Hz), 7.08 (s, 1H), 3.98 (q, 2H, *J* = 6.4 Hz), 1.12 (t, 3H, *J* = 6.4 Hz). LC/MS (APCI⁺) *m/z* 221.2 (MH⁺).

4.1.2.2. Ethyl 4-(4-bromophenyl)-2-hydroxy-4-oxo-2-butenolate (4). White solid (74%); mp 65–66 °C; $^1\text{H NMR}$ (DMSO- d_6) δ 10.68 (s, 1H), 8.07–7.88 (m, 4H), 6.99 (s, 1H), 4.42 (q, 2H, $J = 7.2$ Hz), 1.47 (t, 3H, $J = 7.2$ Hz). LC/MS (APCI $^+$) m/z 299.1 (MH) and 301.2 (MH $^{2+}$).

4.1.2.3. Ethyl 4-biphen-4-yl-2-hydroxy-4-oxo-but-2-enoate (5). Yellow solid (78%); mp 111–112 °C; $^1\text{H NMR}$ (DMSO- d_6) δ 10.68 (s, 1H), 8.10 (d, 2H, $J = 8.8$ Hz), 7.76 (d, 2H, $J = 8.8$ Hz), 7.70–7.64 (m, 2H), 7.55 (m, 3H), 7.15 (s, 1H), 4.46 (q, 2H, $J = 7.2$ Hz), 1.47 (t, 3H, $J = 7.2$ Hz). LC/MS (APCI $^+$) m/z 297.3 (MH $^+$).

4.1.2.4. Ethyl 2-hydroxy-4-oxo-4-phenantr-2-yl-but-2-enoate (6). Yellow solid (85%); mp 116–117 °C; $^1\text{H NMR}$ (DMSO- d_6) δ 10.68 (s, 1H), 8.77 (d, 1H, $J = 8.8$ Hz), 8.74–8.70 (m, 1H), 8.55 (s, 1H), 8.22 (dd, 1H, $J = 8.8$ Hz, $J = 1.8$ Hz), 7.97–7.93 (m, 1H), 7.84 (m, 2H), 7.77–7.67 (m, 2H), 7.27 (s, 1H), 4.46 (q, 2H, $J = 7.2$ Hz), 1.47 (t, 3H, $J = 7.2$ Hz). LC/MS (APCI $^+$) m/z 321.4 (MH $^+$).

4.1.2.5. Ethyl 2-hydroxy-4-napht-2-yl-4-oxo-but-2-enoate (7). Yellow solid (74%); mp 79–80 °C; $^1\text{H NMR}$ (DMSO- d_6) δ 10.68 (s, 1H), 8.57 (s, 1H), 8.07–7.88 (m, 4H), 7.68–7.55 (m, 2H), 7.25 (s, 1H), 4.42 (q, 2H, $J = 7.2$ Hz), 1.47 (t, 3H, $J = 7.2$ Hz). LC/MS (APCI $^+$) m/z 271.3 (MH $^+$).

4.1.2.6. Ethyl 2-hydroxy-4-oxo-4-p-tolyl-but-2-enoate (8). Orange solid (57%); mp 47–48 °C; $^1\text{H NMR}$ (DMSO- d_6) δ 10.68 (s, 1H), 7.97 (d, 2H, $J = 8.2$ Hz), 7.38 (d, 2H, $J = 8.2$ Hz), 7.09 (s, 1H), 4.30 (q, 2H, $J = 7.1$ Hz), 2.37 (s, 1H), 1.31 (t, 3H, $J = 7.0$ Hz). LC/MS (APCI $^+$) m/z 235.3 (MH $^+$).

4.1.2.7. Ethyl 2-hydroxy-4-oxo-4-(4-trifluoromethyl-phenyl)-but-2-enoate (9). Yellow solid (99%); mp 50–51 °C; $^1\text{H NMR}$ (DMSO- d_6) δ 10.68 (s, 1H), 8.02 (d, 2H, $J = 8.2$ Hz), 7.64 (d, 2H, $J = 8.2$ Hz), 6.98 (s, 1H), 4.30 (q, 2H, $J = 7.3$ Hz), 1.30 (t, 3H, $J = 7.3$ Hz). LC/MS (APCI $^+$) m/z 289.2 (MH $^+$).

4.1.2.8. Ethyl 4-biphen-2-yl-2-hydroxy-4-oxo-but-2-enoate (10). Brown solid (37%); mp 63–64 °C; $^1\text{H NMR}$ (DMSO- d_6) δ 10.68 (s, 1H), 7.74–7.31 (m, 10H), 4.35 (q, 2H, $J = 7.2$ Hz), 1.14 (t, 3H, $J = 7.1$ Hz). LC/MS (APCI $^+$) m/z 297.3 (MH $^+$).

4.1.2.9. Ethyl 4-biphen-3-yl-2-hydroxy-4-oxo-but-2-enoate (11). Brown solid (83%); mp 75–76 °C; $^1\text{H NMR}$ (DMSO- d_6) δ 10.68 (s, 1H), 8.08–6.73 (m, 10H), 4.29 (q, 2H, $J = 7.0$ Hz), 1.27 (m, 3H). LC/MS (APCI $^+$) m/z 297.3 (MH $^+$).

4.1.3. General procedure for the preparation of ethyl 5-aryl-isoxazole-3-carboxylate (12–20)

A solution of compound **3–11** (1 equiv) and hydroxylamine hydrochloride (1 equiv) in absolute EtOH was stirred and refluxed for 2 h. At the end of the reaction, the solvent was removed and the residue was purified by flash chromatography cyclohexane/AcOEt (8:2, v/v) followed by crystallization in absolute EtOH.

4.1.3.1. Ethyl 5-phenyl-isoxazole-3-carboxylate (12). White solid (82%); mp 59–60 °C; $^1\text{H NMR}$ (DMSO- d_6) δ 7.52–7.48 (m, 5H), 7.13 (s, 1H), 4.29 (q, 2H, $J = 7.3$ Hz), 1.30 (t, 3H, $J = 7.2$ Hz). LC/MS (APCI $^+$) m/z 218.2 (MH $^+$).

4.1.3.2. Ethyl 5-(4-bromo-phenyl)-isoxazole-3-carboxylate (13). White solid (85%); mp 133–134 °C; $^1\text{H NMR}$ (DMSO- d_6) δ 7.93 (d, 2H, $J = 8.5$ Hz), 7.78 (d, 2H, $J = 8.5$ Hz), 7.58 (s, 1H), 4.39 (q, 2H, $J = 7.1$ Hz), 1.34 (t, 3H, $J = 7.1$ Hz). LC/MS (APCI $^+$) m/z 296.1 (MH) and 298.2 (MH $^{2+}$).

4.1.3.3. Ethyl 5-biphen-4-yl-isoxazole-3-carboxylate (14). White solid (87%); mp 117–118 °C; $^1\text{H NMR}$ (DMSO- d_6) δ 8.30 (d, 2H, $J = 8.5$ Hz), 7.75 (d, 2H, $J = 8.5$ Hz), 7.48–7.46 (m, 3H), 7.25 (d, 2H, $J = 8.5$ Hz), 7.15 (s, 1H), 4.35 (q, 2H, $J = 7.2$ Hz), 1.32 (t, 3H, $J = 7.2$ Hz). LC/MS (APCI $^+$) m/z 294.4 (MH $^+$).

4.1.3.4. Ethyl 5-phenanthren-2-yl-isoxazole-3-carboxylate (15). Yellow solid (90%); mp 196–197 °C; $^1\text{H NMR}$ (DMSO- d_6) δ 8.75 (d, 2H, $J = 6.4$ Hz), 8.65 (s, 1H), 8.24 (d, 1H, $J = 9.0$ Hz), 8.13 (m, 2H), 8.00 (d, 1H, $J = 8.7$ Hz), 7.65 (s, 1H), 7.59–7.56 (m, 2H), 4.42 (q, 2H, $J = 7.3$ Hz), 1.37 (t, 3H, $J = 7.0$ Hz). LC/MS (APCI $^+$) m/z 318.4 (MH $^+$).

4.1.3.5. Ethyl 5-napht-2-yl-isoxazole-3-carboxylate (16). White solid (92%); mp 107–108 °C; $^1\text{H NMR}$ (DMSO- d_6) δ 8.60 (s, 1H), 8.11–8.06 (m, 3H), 8.03–7.98 (m, 1H), 7.64–7.62 (m, 2H), 7.61 (s, 1H), 4.41 (q, 2H, $J = 7.0$ Hz), 1.37 (t, 3H, $J = 7.1$ Hz). LC/MS (APCI $^+$) m/z 268.3 (MH $^+$).

4.1.3.6. Ethyl 5-p-tolyl-isoxazole-3-carboxylate (17). White solid (86%); mp 59–60 °C; $^1\text{H NMR}$ (DMSO- d_6) δ 7.84 (d, 2H, $J = 8.2$ Hz), 7.42 (s, 1H), 7.37 (d, 2H, $J = 8.0$ Hz), 4.38 (q, 2H, $J = 7.1$ Hz), 2.37 (s, 3H), 1.34 (t, 3H, $J = 7.1$ Hz). LC/MS (APCI $^+$) m/z 232.3 (MH $^+$).

4.1.3.7. Ethyl 5-(4-trifluoromethyl-phenyl)-isoxazole-3-carboxylate (18). White solid (73%); mp 136–137 °C; $^1\text{H NMR}$ (DMSO- d_6) δ 8.42 (d, 2H, $J = 8.2$ Hz), 8.36 (d, 2H, $J = 8.2$ Hz), 7.85 (s, 1H), 4.39 (q, 2H, $J = 7.2$ Hz), 1.38 (t, 3H, $J = 7.2$ Hz). LC/MS (APCI $^+$) m/z 286.2 (MH $^+$).

4.1.3.8. Ethyl 5-biphen-2-yl-isoxazole-3-carboxylate (19). White solid (74%); mp 72–73 °C; $^1\text{H NMR}$ (CDCl $_3$) δ 7.89 (d, 1H, $J = 7.0$ Hz), 7.55–7.51 (m, 2H), 7.49–7.40 (m, 4H), 7.30–7.25 (m, 2H), 5.90 (s, 1H), 4.38 (q, 2H, $J = 7.3$ Hz), 1.39 (t, 3H, $J = 7.3$ Hz). LC/MS (APCI $^+$) m/z 294.4 (MH $^+$).

4.1.3.9. Ethyl 5-biphen-3-yl-isoxazole-3-carboxylate (20). White solid (60%); mp 75–76 °C; $^1\text{H NMR}$ (DMSO- d_6) δ 8.26 (s, 1H), 7.96–7.42 (m, 8H), 7.78 (s, 1H), 4.42 (q, 2H, $J = 7.3$ Hz), 1.36 (t, 3H, $J = 7.2$ Hz). LC/MS (APCI $^+$) m/z 294.4 (MH $^+$).

4.1.4. General procedure for the preparation of 5-aryl-isoxazole-3-carboxylic acid (21–29)

To a stirred solution of ester **12–20** (1 equiv) in EtOH (95%), was added sodium hydroxide in pellets (10 equiv). The mixture was then stirred at room temperature for 24 h. EtOH was removed under reduced pressure and the residue was acidified (1N HCl, pH 2) and extracted with EtOAc. The organic extracts were washed with water and brine, dried over MgSO $_4$ and concentrated under reduced pressure to afford essentially pure carboxylic acid **21–29**.

4.1.4.1. 5-Phenyl-isoxazole-3-carboxylic acid (21). White solid (79%); mp 163–164 °C; $^1\text{H NMR}$ (DMSO- d_6) δ 12.79 (s, 1H), 7.96–7.93 (m, 2H), 7.59–7.53 (m, 3H), 7.41 (s, 1H). LC/MS (APCI $^+$) m/z 190.2 (MH $^+$).

4.1.4.2. 5-(4-Bromo-phenyl)-isoxazole-3-carboxylic acid (22). White solid (83%); mp 226–227 °C; $^1\text{H NMR}$ (DMSO- d_6) δ 12.81 (s, 1H), 7.89 (d, 2H, $J = 8.1$ Hz), 7.76 (d, 2H, $J = 8.0$ Hz), 7.48 (s, 1H). LC/MS (APCI $^+$) m/z 268.1 (MH) and 270.2 (MH $^{2+}$).

4.1.4.3. 5-Biphen-4-yl-isoxazole-3-carboxylic acid (23). Yellow solid (61%); mp 212–213 °C; $^1\text{H NMR}$ (DMSO- d_6) δ 12.80 (s, 1H), 8.30 (d, 2H, $J = 8.1$ Hz), 7.75 (d, 2H, $J = 8.5$ Hz),

7.48–7.46 (m, 3H), 7.38 (s, 1H), 7.25 (d, 2H, $J = 8.2$ Hz). LC/MS (APCI⁺) m/z 266.3 (MH⁺).

4.1.4.4. 5-Phenanthr-2-yl-isoxazole-3-carboxylic acid (24). Yellow solid (84%); mp 220–221 °C; ¹H NMR (DMSO-*d*₆) δ 12.81 (s, 1H), 8.75 (d, 1H, $J = 8.2$ Hz), 8.66 (s, 1H), 8.23 (d, 2H, $J = 8.3$ Hz), 8.12 (m, 2H), 8.02 (m, 1H), 7.60–7.57 (m, 2H), 7.54 (s, 1H). LC/MS (APCI⁺) m/z 290.3 (MH⁺).

4.1.4.5. 5-Napht-2-yl-isoxazole-3-carboxylic acid (25). White solid (84%); mp 208–209 °C; ¹H NMR (DMSO-*d*₆) δ 12.79 (s, 1H), 8.57 (s, 1H), 8.09–7.97 (m, 4H), 7.63–7.58 (m, 2H), 7.53 (s, 1H). LC/MS (APCI⁺) m/z 240.2 (MH⁺).

4.1.4.6. 5-*p*-Tolyl-isoxazole-3-carboxylic acid (26). Beige solid (91%); mp 165–166 °C; ¹H NMR (DMSO-*d*₆) δ 12.81 (s, 1H), 7.82 (d, 2H, $J = 8.2$ Hz), 7.35 (d, 2H, $J = 8.2$ Hz), 7.31 (s, 1H), 2.36 (s, 1H). LC/MS (APCI⁺) m/z 204.2 (MH⁺).

4.1.4.7. 5-(4-Trifluoromethyl-phenyl)-isoxazole-3-carboxylic acid (27). White solid (87%); mp 201–202 °C; ¹H NMR (DMSO-*d*₆) δ 12.80 (s, 1H), 8.17 (d, 2H, $J = 7.9$ Hz), 7.93 (d, 2H, $J = 7.9$ Hz), 7.62 (s, 1H). LC/MS (APCI⁺) m/z 258.2 (MH⁺).

4.1.4.8. 5-Biphen-2-yl-isoxazole-3-carboxylic acid (28). White solid (88%); mp 110–111 °C; ¹H NMR (DMSO-*d*₆) δ 12.79 (s, 1H), 7.82 (d, 2H, $J = 6.1$ Hz), 7.60–7.40 (m, 5H), 7.24 (m, 2H), 6.27 (s, 1H). LC/MS (APCI⁺) m/z 266.3 (MH⁺).

4.1.4.9. 5-Biphen-3-yl-isoxazole-3-carboxylic acid (29). White solid (75%); mp 180–181 °C; ¹H NMR (DMSO-*d*₆) δ 12.79 (s, 1H), 8.23 (s, 1H), 7.93 (d, 1H, $J = 7.9$ Hz), 7.84–7.41 (m, 7H), 7.61 (s, 1H). LC/MS (APCI⁺) m/z 266.3 (MH⁺).

4.1.5. General procedure for the preparation of 5-aryl-isoxazole-3-carboxamide (30–48)

To a solution of carboxylic acid **21–29** (1 equiv) in anhydrous CH₂Cl₂ were successively added HBTU (1.5 equiv), HOBT (0.5 equiv) and DIPEA (2 equiv). The mixture was stirred for 45 min at room temperature. Then, the appropriate amine (1.1 equiv) was introduced and the stirring was continued for 24 h. At the end of the reaction, the mixture was filtered off and the filtrate was successively washed with saturated aqueous NaHCO₃ solution, 1N aqueous HCl and distilled water. The organic layer was dried over MgSO₄ and was concentrated in vacuo. The resulting residue was purified by TLC (cyclohexane/AcOEt, 7:3) and crystallized in absolute EtOH to give carboxamide **30–48**.

4.1.5.1. 5-Phenyl-N-(3-phenylpropyl)isoxazole-3-carboxamide (30). White solid (67%); mp 127–128 °C; ¹H NMR (DMSO-*d*₆) δ 8.85 (t, 1H, $J = 5.5$ Hz), 7.93 (d, 2H, $J = 8.2$ Hz), 7.91–7.53 (m, 3H), 7.31 (s, 1H), 7.28–7.14 (m, 5H), 3.29 (t, 2H, $J = 5.8$ Hz), 2.62 (t, 2H, $J = 7.6$ Hz), 1.83 (m, 2H). LC/MS (APCI⁺) m/z 307.2 (MH⁺); Anal. Calcd for C₁₉H₁₈N₂O₂: C, 74.49; H, 5.92; N, 9.14. Found: C, 74.22; H, 5.87; N, 9.35.

4.1.5.2. 5-(4-Bromophenyl)-N-(3-phenylpropyl)isoxazole-3-carboxamide (31). White solid (63%); mp 171–172 °C; ¹H NMR (DMSO-*d*₆) δ 10.93 (t, 1H, $J = 5.7$ Hz), 9.94 (d, 2H, $J = 8.7$ Hz), 9.82 (d, 2H, $J = 8.7$ Hz), 9.47 (s, 1H), 9.36–9.20 (m, 5H), 5.34 (t, 2H, $J = 5.7$ Hz), 4.58 (t, 2H, $J = 7.6$ Hz), 3.89 (m, 2H). LC/MS (APCI⁺) m/z 385.1 (MH) and 387.3 (MH²⁺); Anal. Calcd for C₁₉H₁₇BrN₂O₂: C, 59.24; H, 4.45; N, 7.27. Found: C, 59.36; H, 4.33; N, 7.18.

4.1.5.3. 5-(Biphen-4-yl)-N-(3-phenylpropyl)isoxazole-3-carboxamide (32). White solid (52%); mp 142–143 °C; ¹H NMR (DMSO-*d*₆) δ 8.56 (s, 1H), 8.30 (d, 2H, $J = 8.7$ Hz), 7.75 (d, 2H, $J = 8.5$ Hz), 7.48–7.46 (m, 3H), 7.36 (s, 1H), 7.25 (d, 2H, $J = 8.7$ Hz), 7.20–7.17 (m, 5H), 3.18 (q, 2H, $J = 5.5$ Hz), 2.94 (t, 2H, $J = 7.2$ Hz), 2.10 (m, 2H). LC/MS (APCI⁺) m/z 383.3 (MH⁺); Anal. Calcd for C₂₅H₂₂N₂O₂: C, 78.51; H, 5.80; N, 7.32. Found: C, 78.44; H, 5.66; N, 7.45.

4.1.5.4. 5-(Phenanthr-2-yl)-N-(3-phenylpropyl)isoxazole-5-carboxamide (33). Yellow solid (72%); mp 186–187 °C; ¹H NMR (DMSO-*d*₆) δ 8.91 (t, 1H, $J = 5.7$ Hz), 8.74 (d, 2H, $J = 7.9$ Hz), 8.65 (s, 1H), 8.24 (d, 1H, $J = 9.0$ Hz), 8.14–8.11 (m, 2H), 7.99 (d, 1H, $J = 8.7$ Hz), 7.59–7.56 (m, 2H), 7.51 (s, 1H), 7.31–7.15 (m, 5H), 3.31 (q, 2H, $J = 5.5$ Hz), 2.64 (t, 2H, $J = 7.7$ Hz), 1.86 (m, 2H). LC/MS (APCI⁺) m/z 407.2 (MH⁺); Anal. Calcd for C₂₇H₂₂N₂O₂: C, 79.78; H, 5.46; N, 6.89. Found: C, 79.99; H, 5.47; N, 6.85.

4.1.5.5. 5-(Napht-2-yl)-N-(3-phenylpropyl)isoxazole-3-carboxamide (34). White solid (47%); mp 160–161 °C; ¹H NMR (DMSO-*d*₆) δ 8.89 (t, 1H, $J = 5.5$ Hz), 8.56 (s, 1H), 8.08 (d, 2H, $J = 7.9$ Hz), 8.02–7.98 (m, 2H), 7.63–7.61 (m, 2H), 7.46 (s, 1H), 7.29–7.18 (m, 5H), 3.31 (q, 2H, $J = 5.5$ Hz), 2.63 (t, 2H, $J = 7.6$ Hz), 1.85 (m, 2H). LC/MS (APCI⁺) m/z 357.3 (MH⁺); Anal. Calcd for C₂₃H₂₀N₂O₂: C, 77.51; H, 5.66; N, 7.86. Found: C, 77.44; H, 5.60; N, 7.99.

4.1.5.6. 5-*p*-Tolyl-N-(3-phenylpropyl)isoxazole-3-carboxamide (35). White solid (80%); mp 150–151 °C; ¹H NMR (DMSO-*d*₆) δ 8.83 (t, 1H, $J = 5.7$ Hz), 7.81 (d, 2H, $J = 8.2$ Hz), 7.35 (d, 2H, $J = 8.2$ Hz), 7.31–7.17 (m, 6H), 3.27 (q, 2H, $J = 6.9$ Hz), 2.62 (t, 2H, $J = 7.7$ Hz), 2.37 (s, 3H), 1.83 (m, 2H). LC/MS (APCI⁺) m/z 312.2 (MH⁺); Anal. Calcd for C₂₀H₂₀N₂O₂: C, 74.98; H, 6.29; N, 8.74. Found: C, 75.11; H, 5.95 N, 8.69.

4.1.5.7. 5-(4-(Trifluoromethyl)phenyl)-N-(3-phenylpropyl)isoxazole-3-carboxamide (36). White solid (55%); mp 156–157 °C; ¹H NMR (DMSO-*d*₆) δ 8.93 (t, 1H, $J = 5.7$ Hz), 8.15 (d, 2H, $J = 8.2$ Hz), 7.93 (d, 2H, $J = 8.3$ Hz), 7.56 (s, 1H), 7.31–7.15 (m, 5H), 3.28 (q, 2H, $J = 6.9$ Hz), 2.62 (t, 2H, $J = 7.6$ Hz), 1.83 (m, 2H). LC/MS (APCI⁺) m/z 375.4 (MH⁺); Anal. Calcd for C₂₀H₁₇F₃N₂O₂: C, 64.17; H, 4.58; N, 7.48. Found: C, 64.22; H, 4.71; N, 7.22.

4.1.5.8. N-(2-(Benzo[d][1,3]dioxol-5-yl)ethyl)-5-phenyl-isoxazole-3-carboxamide (37). White solid (65%); mp 191–192 °C; ¹H NMR (DMSO-*d*₆) δ 8.56 (t, 1H, $J = 5.5$ Hz), 7.91 (d, 2H, $J = 8.2$ Hz), 7.85–7.74 (m, 3H), 7.56 (s, 1H), 6.93 (d, 1H, $J = 8.5$ Hz), 6.77 (s, 1H), 6.67 (d, 1H, $J = 8.5$ Hz), 6.06 (s, 2H), 3.45 (q, 2H, $J = 6.9$ Hz), 2.81 (t, 2H, $J = 7.1$ Hz). LC/MS (APCI⁺) m/z 337.2 (MH⁺); Anal. Calcd for C₁₉H₁₆N₂O₄: C, 67.85; H, 4.79; N, 8.33. Found: C, 67.77; H, 5.00 N, 8.39.

4.1.5.9. N-(2-(Benzo[d][1,3]dioxol-5-yl)ethyl)-5-(4-bromophenyl)-isoxazole-3-carboxamide (38). White solid (68%); mp 205–206 °C; ¹H NMR (DMSO-*d*₆) δ 8.83 (t, 1H, $J = 5.5$ Hz), 7.87 (d, 2H, $J = 8.7$ Hz), 7.75 (d, 2H, $J = 8.5$ Hz), 7.39 (s, 1H), 6.82–6.81 (m, 2H), 6.68 (d, 1H, $J = 7.9$ Hz), 5.96 (s, 2H), 3.45 (q, 2H, $J = 6.8$ Hz), 2.81 (t, 2H, $J = 7.3$ Hz). LC/MS (APCI⁺) m/z 415.2 (MH) and 417.3 (MH²⁺); Anal. Calcd for C₁₉H₁₅BrN₂O₄: C, 54.96; H, 3.64; N, 6.75. Found: C, 55.01; H, 3.68 N, 6.82.

4.1.5.10. N-(2-(Benzo[d][1,3]dioxol-5-yl)ethyl)-5-(biphen-4-yl)-isoxazole-3-carboxamide (39). White solid (72%); mp 199–200 °C; ¹H NMR (DMSO-*d*₆) δ 8.84 (t, 1H, $J = 5.5$ Hz), 8.02 (d, 2H, $J = 8.5$ Hz), 7.85 (d, 2H, $J = 8.5$ Hz), 7.75 (d, 2H, $J = 7.3$ Hz), 7.51 (t,

2H, $J = 7.4$ Hz), 7.41 (t, 1H, $J = 7.7$ Hz), 7.38 (s, 1H), 6.83–6.81 (m, 2H), 6.69 (d, 1H, $J = 7.9$ Hz), 5.96 (s, 2H), 3.46 (q, 2H, $J = 6.4$ Hz), 2.77 (t, 2H, $J = 7.3$ Hz). LC/MS (APCI⁺) m/z 413.1 (MH⁺); Anal. Calcd for C₂₅H₂₀N₂O₄: C, 72.80; H, 4.89; N, 6.79. Found: C, 72.97; H, 4.77; N, 6.52.

4.1.5.11. *N*-(2-(Benzo[d][1,3]dioxol-5-yl)ethyl)-5-(naph-2-yl)isoxazole-3-carboxamide (40). White solid (31%); mp 204–205 °C; ¹H NMR (DMSO-*d*₆) δ 8.88 (t, 1H, $J = 5.7$ Hz), 8.56 (s, 1H), 8.08 (d, 2H, $J = 7.6$ Hz), 8.02–7.98 (m, 2H), 7.63–7.60 (m, 2H), 7.45 (s, 1H), 6.85–6.83 (m, 2H), 6.69 (d, 1H, $J = 7.7$ Hz), 5.96 (s, 2H), 3.47 (q, 2H, $J = 6.7$ Hz), 2.79 (t, 2H, $J = 7.3$ Hz). LC/MS (APCI⁺) m/z 387.2 (MH⁺); Anal. Calcd for C₂₃H₁₈N₂O₄: C, 71.49; H, 4.70; N, 7.25. Found: C, 71.22; H, 4.81; N, 7.53.

4.1.5.12. *N*-(2-(Benzo[d][1,3]dioxol-5-yl)ethyl)-5-*p*-tolyl-isoxazole-3-carboxamide (41). White solid (45%); mp 187–188 °C; ¹H NMR (DMSO-*d*₆) δ 8.79 (t, 1H, $J = 5.4$ Hz), 7.80 (d, 2H, $J = 8.2$ Hz), 7.35 (d, 2H, $J = 8.2$ Hz), 7.25 (s, 1H), 6.83–6.81 (m, 2H), 6.67 (d, 1H, $J = 7.9$ Hz), 5.96 (s, 2H), 3.44 (q, 2H, $J = 6.5$ Hz), 2.76 (t, 2H, $J = 7.3$ Hz), 2.37 (s, 3H). LC/MS (APCI⁺) m/z 351.4 (MH⁺); Anal. Calcd for C₂₀H₁₈N₂O₄: C, 68.56; H, 5.18; N, 8.00. Found: C, 68.72; H, 5.02; N, 7.88.

4.1.5.13. *N*-(2-(Benzo[d][1,3]dioxol-5-yl)ethyl)-5-(4-(trifluoromethyl)phenyl)isoxazole-3-carboxamide (42). White solid (38%); mp 187–188 °C; ¹H NMR (DMSO-*d*₆) δ 8.89 (t, 1H, $J = 5.8$ Hz), 8.15 (d, 2H, $J = 8.2$ Hz), 7.92 (d, 2H, $J = 8.2$ Hz), 7.54 (s, 1H), 6.81 (m, 2H), 6.68 (d, 1H, $J = 8.2$ Hz), 5.96 (s, 2H), 3.45 (q, 2H, $J = 6.7$ Hz), 2.77 (t, 2H, $J = 7.3$ Hz). LC/MS (APCI⁺) m/z 405.3 (MH⁺); Anal. Calcd for C₂₀H₁₅F₃N₂O₄: C, 59.41; H, 3.74; N, 6.93. Found: C, 59.28; H, 3.88; N, 7.03.

4.1.5.14. *N*-(2-(Benzo[d][1,3]dioxol-5-yl)ethyl)-5-(biphen-2-yl)isoxazole-3-carboxamide (43). White solid (18%); mp 137–138 °C; ¹H NMR (DMSO-*d*₆) δ 8.44 (t, 1H, $J = 7.2$ Hz), 7.79 (m, 2H), 7.54–7.28 (m, 8H), 6.93–6.77 (m, 3H), 6.07 (s, 2H), 3.49 (q, 2H, $J = 6.4$ Hz), 2.81 (t, 2H, $J = 7.2$ Hz). LC/MS (APCI⁺) m/z 413.1 (MH⁺); Anal. Calcd for C₂₅H₂₀N₂O₄: C, 72.80; H, 4.89; N, 6.79. Found: C, 72.66; H, 4.95; N, 6.55.

4.1.5.15. *N*-(2-(Benzo[d][1,3]dioxol-5-yl)ethyl)-5-(biphen-3-yl)isoxazole-3-carboxamide (44). White solid (64%); mp 149–150 °C; ¹H NMR (DMSO-*d*₆) δ 8.76 (t, 1H, $J = 7.2$ Hz), 8.21 (s, 1H), 7.93–7.39 (m, 9H), 6.82 (s, 1H), 6.72–6.69 (m, 2H), 5.96 (s, 2H), 3.46 (q, 2H, $J = 6.4$ Hz), 2.77 (t, 2H, $J = 7.3$ Hz). LC/MS (APCI⁺) m/z 413.1 (MH⁺); Anal. Calcd for C₂₅H₂₀N₂O₄: C, 72.80; H, 4.89; N, 6.79. Found: C, 72.92; H, 5.01; N, 6.48.

4.1.5.16. 5-(Biphen-4-yl)-*N*-(3-benzyl)isoxazole-3-carboxamide (45). White solid (31%); mp 195–196 °C; ¹H NMR (DMSO-*d*₆) δ 9.40 (t, 1H, $J = 6.1$ Hz), 8.02 (d, 2H, $J = 8.4$ Hz), 7.85 (d, 2H, $J = 8.2$ Hz), 7.75 (d, 2H, $J = 7.2$ Hz), 7.52–7.23 (m, 9H), 4.47 (d, 2H, $J = 6.4$ Hz). LC/MS (APCI⁺) m/z 355.4 (MH⁺); Anal. Calcd for C₂₃H₁₈N₂O₂: C, 77.95; H, 5.12; N, 7.90. Found: C, 77.78; H, 5.34; N, 7.72.

4.1.5.17. 5-(Biphen-4-yl)-*N*-(3-phenethyl)isoxazole-3-carboxamide (46). White solid (26%); mp 210–211 °C; ¹H NMR (DMSO-*d*₆) δ 8.89 (t, 1H, $J = 5.8$ Hz), 8.00 (d, 2H, $J = 8.2$ Hz), 7.85 (d, 2H, $J = 8.5$ Hz), 7.75 (d, 2H, $J = 7.3$ Hz), 7.53–7.20 (m, 9H), 3.50 (q, 2H, $J = 6.7$ Hz), 2.86 (t, 2H, $J = 7.57$ Hz). LC/MS (APCI⁺) m/z 369.4 (MH⁺); Anal. Calcd for C₂₄H₂₀N₂O₂: C, 78.24; H, 5.47; N, 7.60. Found: C, 78.51; H, 5.72; N, 7.59.

4.1.5.18. *N*-(Benzo[d][1,3]dioxol-5-yl)-5-(biphen-4-yl)isoxazole-3-carboxamide (47). White solid (24%); mp 215–216 °C; ¹H

NMR (DMSO-*d*₆) δ 10.70 (s, 1H), 8.05 (d, 2H, $J = 8.4$ Hz), 7.85 (d, 2H, $J = 8.2$ Hz), 7.76 (d, 2H, $J = 7.0$ Hz), 7.53–7.48 (m, 4H), 6.92–6.81 (m, 3H), 6.02 (s, 2H). LC/MS (APCI⁺) m/z 385.4 (MH⁺); Anal. Calcd for C₂₃H₁₆N₂O₄: C, 71.87; H, 4.20; N, 7.29. Found: C, 71.59; H, 4.44; N, 7.17.

4.1.5.19. *N*-(2-(Benzo[d][1,3]dioxol-5-yl)methyl)-5-(biphen-4-yl)isoxazole-3-carboxamide (48). White solid (17%); mp 197–198 °C; ¹H NMR (DMSO-*d*₆) δ 9.34 (t, 1H, $J = 6.1$ Hz), 8.02 (d, 2H, $J = 8.4$ Hz), 7.85 (d, 2H, $J = 8.2$ Hz), 7.75 (d, 2H, $J = 7.3$ Hz), 7.52–7.39 (m, 4H), 6.91–6.80 (m, 3H), 5.98 (s, 2H), 4.35 (d, 2H, $J = 6.1$ Hz). LC/MS (APCI⁺) m/z 399.4 (MH⁺); Anal. Calcd for C₂₄H₁₈N₂O₄: C, 72.35; H, 4.55; N, 7.03. Found: C, 72.21; H, 4.58; N, 7.11.

4.2. In vitro assays towards human FAAH and MAGL

Tubes containing human recombinant FAAH (expressed in *E. Coli*) in buffer (100 mM Tris-HCl, 1 mM EDTA, 0.1% (w/v) BSA, pH 7.4, 165 μ L), test compounds in DMSO, or DMSO alone for controls (10 μ L), and [³H]-AEA (50 000 dpm, 2 μ M final concentration, 25 μ L) were incubated at 37 °C for 10 min. Reactions were stopped by rapidly adding 400 μ L of ice-cold chloroform/methanol (1:1 v/v) followed by vigorous mixing. Phases were separated by centrifugation at 850 \times g, and aliquots (200 μ L) of the upper methanol/buffer phase were counted for radioactivity by liquid scintillation. In all experiments, tubes containing buffer only were used as control for chemical hydrolysis (blank) and this value was systematically subtracted. Using these conditions, the well known FAAH inhibitor URB597 inhibits hFAAH with an IC₅₀ value of 40 nM. MAGL inhibition was assayed using a similar protocol but with purified hMAGL and [³H]-2-OG (10 μ M) instead of FAAH and [³H]-AEA, respectively.²⁰

4.3. In vivo Assays

C57Bl6 mice ($n = 10$ per group) had free access to standard mouse chow and tap water. For colitis induction, mice were anesthetized by subcutaneous administration of xylazine-ketamine (50 mg/kg) in saline for 90–120 min and received an intrarectal administration of TNBS (40 μ L, 150 mg/kg) dissolved in a 1:1 mixture of 0.9% NaCl with 100% ethanol. Control mice ($n = 6$) received a 1:1 mixture of 0.9% NaCl with 100% ethanol using the same technique. 5-ASA granules mixed in food at the dosage of 150 mg/kg and provided ad libitum during all the course of the experiment was used as anti-inflammatory positive control. The FAAH inhibitor **39** was dissolved in vehicle (DMSO 2%, Tween 80 1% in saline) and administered intraperitoneally once daily, starting three days before colitis induction at the dosage of 10 mg/kg. Animals were euthanized three days after TNBS administration. Body-weight changes, macroscopic and histological indications of colitis were evaluated blindly by two investigators. The colon of each mouse was examined to evaluate the macroscopic lesions according to the Wallace criteria.²³ The Wallace score rates macroscopic lesions on a scale from 0 to 10 based on features reflecting inflammation, such as hyperemia, thickening of the bowel, and extent of ulceration. A colon specimen located precisely 2 cm above the anal canal was used for histological evaluation following May-Grunwald Giemsa staining and according to the Ameho criteria.²⁴ This grading on a scale from 0 to 6 takes into account the degree of inflammation infiltrate, the presence of erosion, ulceration, or necrosis, and the depth and surface extension of lesions. The other parts of the colon were frozen and used to quantify cytokines mRNA levels.

4.4. Quantification of colonic cytokines levels by real-time PCR

Total RNA from colon was extracted using Nucleospin RNAII (Macherey Nagel, Hoerd, France) and then reverse transcribed using the high-Capacity cDNA Reverse Transcription Kit (Applied Biosystems, Foster City, USA). Real time PCR was performed using SYBR Green (Applied Biosystems, Foster City, USA). Specific primers for TNF (TNFa_F_Sou_MBM; CCACCACGCTCTTCTGTCTA and TNFa_R_Sou_MBM; GAGGCCATTGGGAACCTCT), IL-1 β (IL1 β _F_sou_MBM; AGCTCTCCACCTCAATGGAC and IL1 β _R_Sou_MBM; AGGCCACAGTATTTTGTCC) and β -Actin acting as internal control were designed using the Primer Express Program (Applied Biosystems, Foster City, USA). For graphical representation of quantitative PCR data, raw cycle threshold values (Ct values) obtained for target samples were deducted from the Ct value obtained for internal control transcript levels, using the $\Delta\Delta C_t$ method as follows: $\Delta\Delta C_t = (C_{t,target-Ct,control} - C_{t,target-Ct,control}^{non-treatment})$, and the final data were derived from $2^{-\Delta\Delta C_t}$.

Acknowledgments

The authors thank Ms. Perrine Six for the NMR and LC–MS analysis, as well as Dr. Geoffray Labar for the preparation of the human recombinant enzymes. This work was financially supported by the ‘Conseil Régional Nord Pas de Calais’.

References and notes

- Vandevoorde, S.; Lambert, D. M. *Chem. Biodivers.* **2007**, *4*, 1858.
- Ahn, K.; McKinney, M. K.; Cravatt, B. F. *Chem. Rev.* **2008**, *108*, 1687.
- Dinh, T. P.; Freund, T. F.; Piomelli, D. A. *Chem. Phys. Lipids* **2002**, *121*, 149.
- Muccioli, G. G. *Drug Discovery Today* **2010**, *15*, 474.
- Izzo, A. A.; Sharkey, K. A. *Pharmacol. Ther.* **2010**, *126*, 21.
- D'Argenio, G.; Valenti, M.; Scaglione, G.; Cosenza, V.; Sorrentini, I.; Di Marzo, V. *FASEB J.* **2006**, *20*, 568.
- Wright, K.; Rooney, N.; Feeney, M.; Tate, J.; Robertson, D.; Welham, M.; Ward, S. *Gastroenterology* **2005**, *129*, 437.
- Marqu ez, L.; Su arez, J.; Iglesias, M.; Bermudez-Silva, F. J.; Rodr guez de Fonseca, F.; Andreu, M. *PLoS ONE* **2009**, *4*, e6893.
- Di Marzo, V.; Izzo, A. *Gut* **2006**, *55*, 1373.
- Storr, M. A.; Keenan, C. M.; Zhang, H.; Patel, K. D.; Makriyannis, A.; Sharkey, K. A. *Inflamm. Bowel. Dis.* **2009**, *15*, 1678.
- Storr, M. A.; Keenan, C. M.; Emmerdinger, D.; Zhang, H.; Y uce, B.; Sibae, A.; Massa, F.; Buckley, N. E.; Lutz, B.; G oke, B.; Brand, S.; Patel, K. D.; Sharkey, K. A. *J. Mol. Med.* **2008**, *86*, 925.
- Massa, F.; Marsicano, G.; Hermann, H.; Cannich, A.; Monory, K.; Cravatt, B. F.; Ferri, G. L.; Sibae, A.; Storr, M.; Lutz, B. *J. Clin. Invest.* **2004**, *113*, 1202.
- Cravatt, B. F.; Lichtman, A. H. *Curr. Opin. Chem. Biol.* **2003**, *7*, 469.
- Garfinkle, J.; Ezzili, C.; Rayl, T. J.; Hochstatter, D. G.; Hwang, I.; Boger, D. L. *J. Med. Chem.* **2008**, *51*, 4392.
- Mor, M.; Lodola, A.; Rivara, S.; Vacondio, F.; Duranti, A.; Tontini, A.; Sanchini, S.; Piersanti, G.; Clapper, J. R.; King, A. R.; Tarzia, G.; Piomelli, D. *J. Med. Chem.* **2008**, *51*, 3487.
- Seierstad, M.; Breitenbucher, J. G. *J. Med. Chem.* **2008**, *51*, 7327.
- Andrzejak, V.; Millet, R.; El Bakali, J.; Guelzim, A.; Gluszk, S.; Chavatte, P.; Bonte, J. P.; Vaccher, C.; Lipka, E. *Lett. Org. Chem.* **2010**, *7*, 32.
- Labar, G.; Vliet, F. V.; Wouters, J.; Lambert, D. M. *Amino Acids* **2008**, *34*, 127.
- Muccioli, G. G.; Labar, G.; Lambert, D. M. *Chem. Biol. Chem.* **2008**, *9*, 2704.
- Muccioli, G. G.; Fazio, N.; Scriba, G. K.; Poppitz, W.; Cannata, F.; Poupaert, J. H.; Wouters, J.; Lambert, D. M. *J. Med. Chem.* **2006**, *49*, 417.
- Ritland, S. R.; Leighton, J. A.; Hirsch, R. E.; Morrow, J. D.; Weaver, A. L.; Gendler, S. *Clin. Cancer Res.* **1999**, *5*, 855.
- Wallace, J. L.; MacNaughton, W. K.; Morris, G. P.; Beck, P. L. *Gastroenterology* **1989**, *96*, 29.
- Ameho, C. K.; Adjei, A. A.; Harrison, E. K.; Takeshita, K.; Morioka, T.; Arakaki, Y.; Ito, E.; Suzuki, I.; Kulkarni, A. D.; Kawajiri, A.; Yamamoto, S. *Gut* **1997**, *41*, 487.
- Mileni, M.; Garfinkle, J.; DeMartino, J. K.; Cravatt, B. F.; Boger, D. L.; Stevens, R. C. *J. Am. Chem. Soc.* **2009**, *131*, 10497.
- Jones, G.; Willett, P.; Glen, R. C.; Leach, A. R.; Taylor, R. *J. Mol. Biol.* **1997**, *267*, 727.
- Katritch, V.; Byrd, C. M.; Tsetin, V.; Dai, D.; Raush, E.; Totrov, M.; Abagyan, R.; Jordan, R.; Hruba, D. E. *J. Comput.-Aided Mol. Des.* **2007**, *21*, 549.
- Tripos Associates, Inc., 1699 South Hanley Road, St. Louis, MO 63144.